DOI: 10.1002/smll.200701295

# Shape Control of Colloidal Metal Nanocrystals

*Andrea R. Tao, Susan Habas, and Peidong Yang**

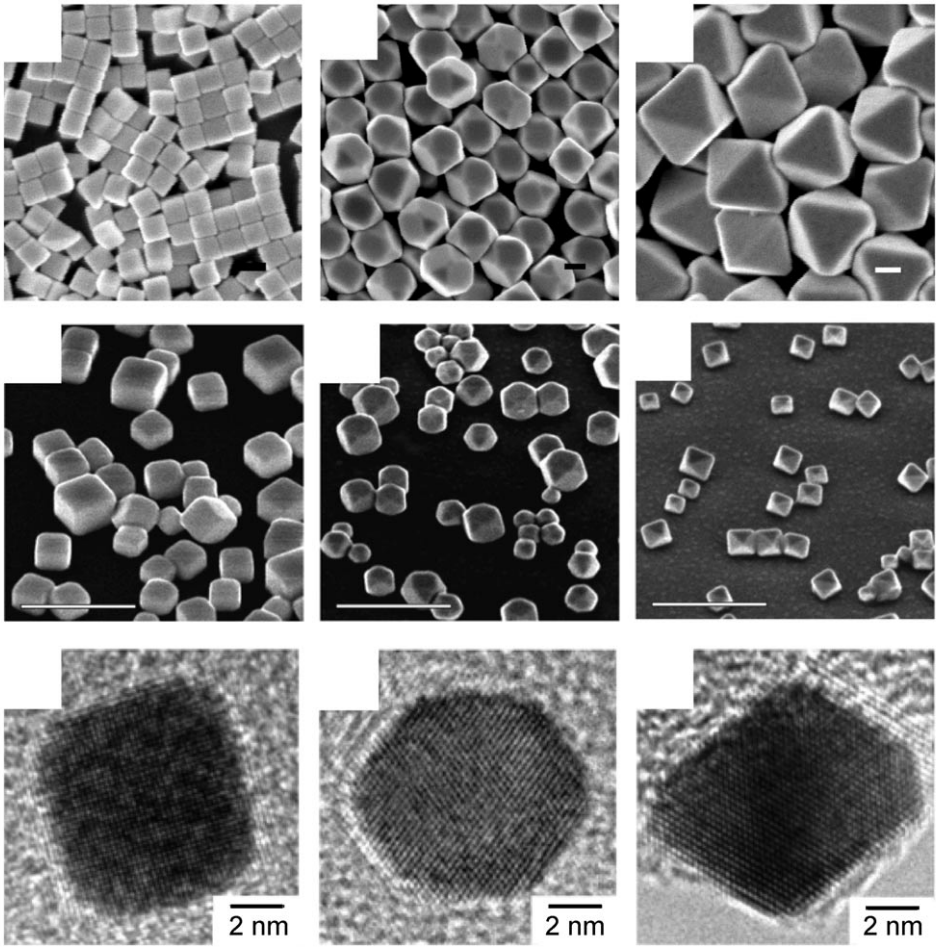


Polyhedral metal nanocrystals.

From the Contents



**Keywords:**
- colloids
- nanocrystals
- nanoparticles
- shape control



© 2008 Wiley-VCH Verlag GmbH & Co. KGaA, Weinheim

NANO MICRO small

*Colloidal metal nanoparticles are emerging as key materials for catalysis, plasmonics, sensing, and spectroscopy. Within these applications, control of nanoparticle shape lends increasing functionality and selectivity. Shape-controlled nanocrystals possess well-defined surfaces and morphologies because their nucleation and growth are controlled at the atomic level. An overall picture of shaped metal particles is presented, with a particular focus on solution-based syntheses for the noble metals. General strategies for synthetic control are discussed, emphasizing key factors that result in anisotropic, nonspherical growth such as crystallographically selective adsorbates and seeding processes.*

## 1. Introduction

The scientific mantra of "structure dictates function" – a tenet largely taught to biologists and biochemists – is quickly being adopted by researchers who deal with materials at the nanoscale. In biology, this catch phrase is exemplified by proteins whose roles in specific chemical pathways are strictly determined by the way these large biomolecules fold or form hierarchical structures based on chemical interactions with themselves or other molecules. To chemists, physicists, and engineers, a similar structure–function relationship is the underlying motive for discovering and characterizing novel nanoscale structures. At this length scale, the properties of a given material may deviate significantly from its bulk counterpart. The archetypal example is the photoluminescent semiconductor quantum dot (nanoparticles composed of semiconducting materials such as CdS with diameters ~1–10 nm) whose emission wavelength can be tuned by varying the nanocrystal radius. New methods of synthesizing nanoscale materials have also shown that in addition to size, a nanostructure's shape can also profoundly affect its physical properties. Nonspherical architectures such as one-dimensional (1D) wires and rods, facetted particles, multipod structures, and shapes with high asymmetry have demonstrated a fascinating variety of properties, such as the polarized light emission of CdSe nanorods or the light-mediated aggregation of triangular Ag prisms[1].

In the case of noble metal nanoparticles such as Ag, Au, Pt, and Pd, this shape dependence is particularly evident. For example, Ag and Au nanocrystals of different shapes possess unique optical scattering responses. Whereas highly symmetric spherical particles exhibit a single scattering peak, anisotropic shapes such as rods[2], triangular prisms[1], and cubes[3] exhibit multiple scattering peaks in the visible wavelengths due to highly localized charge polarizations at corners and edges. Controlling nanocrystal shape thus provides an elegant strategy for optical tuning. Similarly, chemical reactivity is highly dependent on surface morphology. The bounding facets of the nanocrystal, the number of step edges and kink sites, as well as the surface-area-to-volume ratio can dictate unique surface chemistries. For this reason, Pt and Pd nanocrystals exhibit shape- and size-dependent catalytic properties[4] that may prove useful in achieving highly selective catalysis. Optimizing nanocatalyst morphology has become a prolific area of investigation. These exciting possibilities have raised the key question: can we rationally control nanocrystal shape and surface morphology?

For the noble-metal systems, crystallographic control over the nucleation and growth of nanoparticles has been most widely achieved using colloidal methods. In most cases, a metal salt precursor is reduced in solution (aqueous or otherwise) in the presence of a stabilizing agent, which prevents aggregation or improves the chemical stability of the formed nanoparticles. Colloidal methods are advantageous because: 1) No specialized equipment is necessary; 2) solution-based processing and assembly can be readily implemented; 3) large quantities of nanoparticles can be synthesized. These reasons are especially important when considering real applications; in order to utilize metal nanoparticles as optical, electronic, or catalytic materials, large-scale synthesis and assembly is required.

In the absence of a hard template, solution-based methods for producing low-dimensional structures require precise tuning of nucleation and growth steps to achieve crystallographic control. These reactions are governed by thermodynamic (e.g., temperature, reduction potential) and kinetic (e.g., reactant concentration, diffusion, solubility, reaction rate) parameters that are intimately and intricately linked. Thus, the exact mechanisms for shape-controlled colloidal synthesis are often not well understood or characterized. However, some general strategies have emerged after

[*] S. Habas, Prof. P. Yang
Department of Chemistry
University of California
Berkeley, CA 94720 (USA)
Materials Science Division
Lawrence Berkeley National Laboratory
Berkeley, CA 94720 (USA)
Fax: (+1) 510-642-7301
E-mail: p_yang@uclink.berkeley.edu
A. R. Tao
Institute for Collaborative Biotechnologies
University of California, Santa Barbara, CA 93111 (USA)

 © 2008 Wiley-VCH Verlag GmbH & Co. KGaA, Weinheim 

being demonstrated experimentally and are outlined here in the context of noble-metal systems. In this Review, we first discuss the general morphologies exhibited by noble metals, including a brief history of more common nanocrystalline shapes. Due to the large body of literature on this subject, this Review is not intended to be comprehensive, rather, we would like to discuss some salient features of shape-controlled nanocrystal growth using examples mainly from the authors' lab. Shape-controlled synthesis can be grouped into two main categories: homogeneous nucleation or seeded, heterogeneous nucleation. Sections 3 and 4 provide an overview of the different procedures that fall under each category, respectively. Section 5 covers unique applications of shape-controlled metal nanoparticles, including a brief discussion of post-synthesis assembly. Finally, we discuss the outlook of these shaped metal nanoparticles and challenges that must be addressed before their application as functional nanoscale materials.

## 2. Nanoparticle Morphology

Unlike a bulk material, the thermodynamic and kinetic considerations for nanocrystal formation are complicated by the high surface-area-to-volume ratio of particles in this size regime. Because nanocrystals possess finite volumes, strict lattice invariance may not apply. Small metal particles are able to accommodate large amounts of strain, often through the formation of irregular polycrystalline structures and lattice defects.[5] Happily, the morphology of metal surfaces has been a well-studied topic in solid-state chemistry over the past several decades, bearing importance at the fundamental, technological, and aesthetic levels of materials synthesis and application. Equilibrium shapes and thermodynamic effects, in particular, have been extensively probed for particles composed of Ag, Au, and Pt both experimentally and theoretically.[6–9] With improvements in electron microscopy techniques and instrumentation, new experimental insight can also be gained regarding the kinetics of nanocrystal growth.

Surface-energy considerations are crucial in understanding and predicting the morphology of noble-metal nanocrystals. Surface energy, defined as the excess free energy per unit area for a particular crystallographic face, largely determines the faceting and crystal growth observed for particles at both the nano- and mesoscale. For a material with an isotropic surface energy such as an amorphous solid or liquid droplet, total surface energy can be lowered simply by decreasing the amount of surface area corresponding to a given volume. The resulting particle shape is a perfectly symmetric sphere. Noble metals, which adopt a face-centered cubic (fcc) lattice, possess different surface energies for different crystal planes. This anisotropy results in stable morphologies where free energy is minimized by particles bound by the low-index crystal planes that exhibit closest atomic packing. For Ag at zero temperature, surface-energy calculations predict that any high-index Ag(*hkl*) crystal planes will spontaneously facet into linear combinations of the low-index {111}, {100}, and {110} planes.[7] Similar theoretical results were obtained for single-crystalline structures of Cu, Ni, Pd, Pt, and Au, predicting the instability and subsequent reconstruction of all high-index fcc crystal planes. Clean low-index surfaces of 5d fcc metals (Pt, Au) exhibit extensive surface reconstructions, where the top atomic


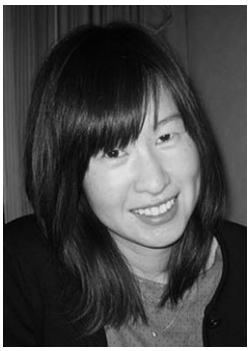

Andrea Tao is currently a postdoctoral researcher at the University of California, Santa Barbara, where she holds a UC Office of the President's Postdoctoral Fellowship. She received her A.B. in chemistry and physics from Harvard in 2002 and her Ph.D. in chemistry from UC Berkeley in 2007, where she worked on the synthesis and assembly of nanocrystals for plasmonic applications. Her current research interests include biomimetic composite materials and self-assembling nanoscale systems.

Susan Habas is currently a graduate student in the Peidong Yang group at the University of California, Berkeley. She entered Berkeley in 2001 after receiving her A.B. in chemistry and biochemistry from Wheaton College, and then attended Massey University in New Zealand as a Fulbright Fellow from 2002–2003. Upon returning to Berkeley her research interests have focused on the shape control and selectivity of multimaterial heterostructures for catalytic and energy applications.

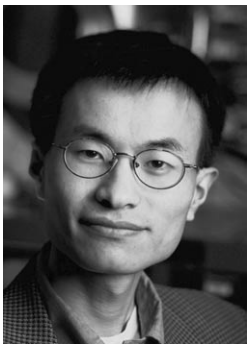

Peidong Yang received a B.S. in chemistry from the University of Science and Technology of China in 1993 and a Ph.D. in chemistry from Harvard University in 1997. He did postdoctoral research at University of California, Santa Barbara, before joining the faculty in the Department of Chemistry at the University of California, Berkeley, in 1999. He is currently professor in the Department of Chemistry, Materials Science, and Engineering, and a faculty scientist at the Lawrence Berkeley National Laboratory. He is the recipient of an Alfred P. Sloan research fellowship, the Arnold and Mabel Beckman Young Investigator Award, the MRS Young Investigator Award, the Julius Springer Prize for Applied Physics, and the ACS Pure Chemistry Award and Alan T. Waterman Award. His main research interest is in the area of one-dimensional semiconductor nanostructures and their applications in nanophotonics, energy conversion, and nanofluidics.


 © 2008 Wiley-VCH Verlag GmbH & Co. KGaA, Weinheim 

small NANO MICRO

layers of the Au(111) and both Au and Pt(100) and (110) crystal planes undergo lattice rearrangement.[10] Thus, in general, noble-metal nanocrystals are exclusively composed of the lowest-index crystal planes although nanocrystals with high-index planes were also recently synthesized using an electrochemical method.[11]

### 2.1. Single-Crystalline Particles

For single-crystalline particles, where the entire volume is composed of only one crystalline domain, the predicted thermodynamic equilibrium shape is a truncated octahedron bound by {111} and {100} planes,[7] as highlighted in Figure 1. In practice, however, kinetic considerations are also critical in determining nanocrystal morphology. This is particularly evident in colloidal syntheses, where parameters such as reaction time, capping agents, and reactant concentration profoundly affect nucleation and growth. Xia et al. were among the first to demonstrate the colloidal shape control of Ag nanocrystals, obtaining kinetically controlled growth of single-crystalline nanocubes bound by {100} crystal facets. In their synthesis, small volumes of $AgNO_3$ solution were injected into a reducing solvent, with injection time and injection volume dictating nucleation events during the reaction.[3] Our group extended this kinetic control to produce a variety of single-crystalline Ag nanocrystals with octahedral ($O_h$) symmetry and bound exclusively by {100} and {111} crystal planes, including cubes, truncated cubes, cuboctahedra, truncated octahedra, and octahedra.[12] Similar cubic, cuboctahedral, and octahedral geometries were also demonstrated with colloidal Pt nanocrystals[13] and in the case of Au colloidal nanocrystals, careful control of reactant concentration and injection rate achieved additional single-crystalline morphologies, such as octahedra[14] and tetrahedra[15] (see Figure 2). In addition, single-crystalline nanoparticles with distinctly non-Wulff shapes that deviate significantly from near-spherical symmetries have been demonstrated, such as 2D Au hexagonal plates,[16] Ag plates,[17,18] nanorods,[19] and dendrites,[20] as depicted in Figure 1.

### 2.2. Multiply Twinned Particles

Some of most common particle morphologies, however, are not composed of single domains but rather possess twin planes, as depicted in Figure 3a. These multiply twinned particles (MTPs) typically exhibit near-fivefold symmetries and were observed as early as the 1960s, with actual twinned crystal structures confirmed later by high-resolution transmission electron microscopy (HRTEM).[6] The most commonly observed polyhedra are the decahedron (10 faces) and the icosahedron (20 faces), with both shapes exclusively bound by the (111) fcc crystal planes, shown in Figure 3b and c, respectively. The formation of MTPs for Ag, Au, Cu, Pt, and Pd is attributed to the low twinning energies of these noble metals, which can accommodate the strain induced by a completely (111)-bound particle. The Mackay Icosahedron, named after the scientist who constructed the polyhedron from a close-packed assembly of spheres,[21] is an equilibrium shape bound entirely by 20 triangular (111) facets with 12 vertices and 30 edges. For the fcc noble metals, this produces a highly strained structure with significant energetic contributions from this distorted internal lattice. Thus, despite minimization of surface energy due to the presence of (111) facets, icosahedra are only predicted for smaller clusters typically ob-

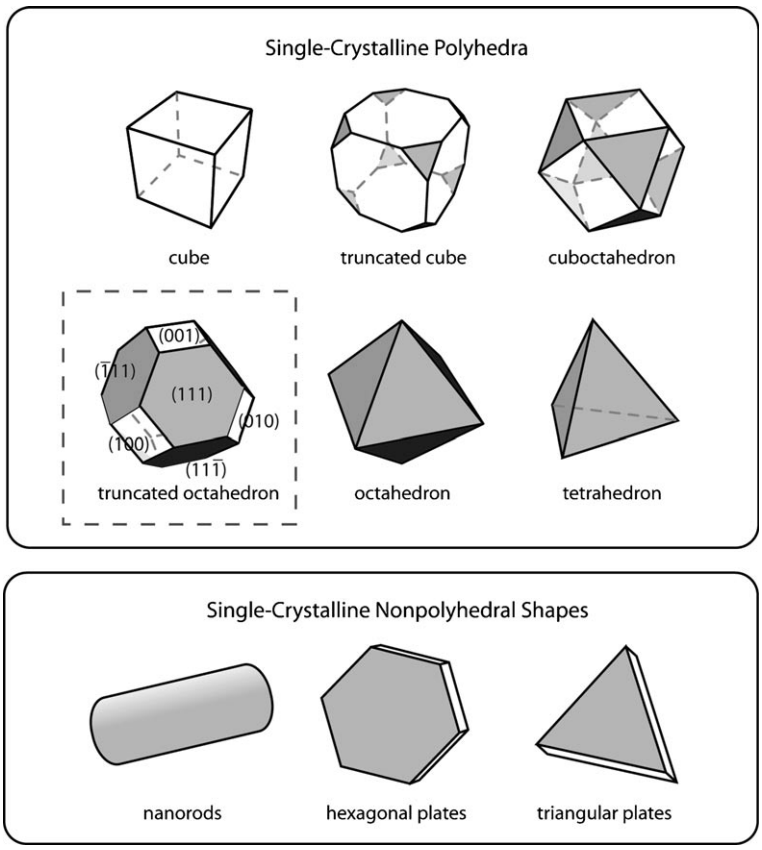


**Figure 1.** Common morphologies of single-crystalline metal nanoparticles. Polyhedral shapes (top) with octahedral symmetries where each shape can be transformed into another by truncation of its corners. Nonpolyhedral shapes (bottom) are mostly composed of anisotropic structures with small aspect ratios or large platelike structures.

 © 2008 Wiley-VCH Verlag GmbH & Co. KGaA, Weinheim 

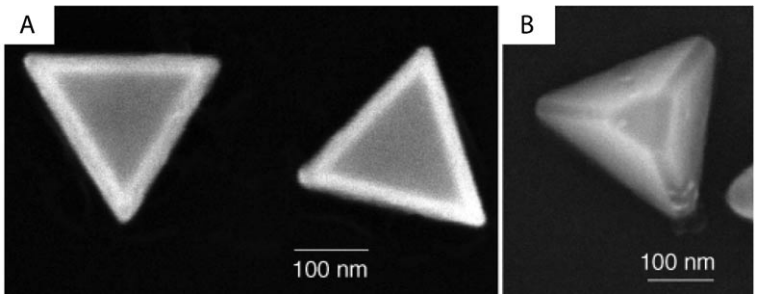


**Figure 2.** Tetrahedral gold nanocrystals obtained with the polyol synthesis. A) Truncated tetrahedra and B) an almost complete tetrahedron displaying strong corner and edge faceting (adapted from Reference [15]).

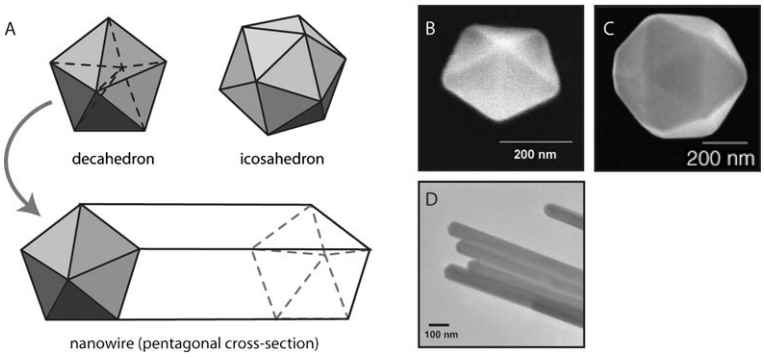


**Figure 3.** Metal nanocrystals exhibiting twin planes. A) Schematic image of the commonly observed decahedron and the less common icosahedron. Nanowires possessing fivefold cross-section symmetries result from anisotropic crystal growth onto a decrahedral seed particle. B–D) Electron microscopy images of gold nanocrystals and silver nanowires exemplifying the aforementioned shapes (adapted from References [15, 85]).

served in gas-phase syntheses at high temperatures.[22] Monodisperse samples of larger colloidal icosahedra have been observed only rarely in the Au and Pd systems.[15,23,24] A more commonly observed shape for colloidal noble-metal particles is the decahedron. A regular decahedron is an equilibrium shape bound completely by triangular (111) facets and can be thought of as five tetrahedra sharing a common edge along a fivefold axis. Like the icosahedron, the decahedron is a strained structure but possesses a slightly more efficient space-filling structure. These structures are commonly observed for nanoscale particles synthesized by metal evaporation onto solid substrates[25] and seeded solutions.[26]

For nanocrystals synthesized in colloidal solutions, however, decahedra are difficult to observe in situ as they behave as favorable seeds for the growth of 1D structures. Nanowires and nanorods, as shown in Figure 3d, possessing fivefold pentagonal cross sections, have been observed for Au, Ag, and Pd and are believed to result from anisotropic growth onto decahedral seed particles.[23,27,28] This growth mechanism, which has been observed to occur for a variety of colloidal systems and capping agents, is thought to be encouraged by the high-energy twin plane surfaces exposed at the end vertices of the decahedron, facilitating fast metal reduction with a preferential growth direction. This strategy for anisotropic growth can also be extended for the formation of branched structures by secondary growth on an unstable, twinned, seed particle.[29] Branched and podlike structures have been shown for Pt,[30] Rh,[31–33] and Au.[34] The addition of ionic species such as $Ag^+$ may act to break the symmetry of the fcc crystal through selective interaction with various crystal faces,[13] resulting in anisotropic growth of single-crystalline branched Pt nanoparticles.[35]

## 3. Seed Nucleation

As in the general case for colloidal synthesis, the nucleation process is critical for obtaining shaped metal nanoparticles. The formation or addition of small seed particles – particles that serve as nucleation sites for metal reduction – can not only determine the crystallographic growth of the resulting nanoparticle but can also drastically change the kinetics of nanocrystal growth. Shape control of metal nanocrystals can be carried out via either homogeneous or heterogeneous nucleation. In homogeneous nucleation, seed particles are formed in situ and, typically, nucleation and growth proceed by the same chemical process. This is the more common synthetic strategy due to the practical ease of carrying out a one-pot reaction. Heterogeneous nucleation is carried out by adding preformed seed particles to a reactant mixture, effectively isolating nanocrystal nucleation and growth as separate synthetic steps. Such a strategy is particularly advantageous as it allows thoughtful design of nanocrystal shape through the choice of seed particles. In this section, we look more closely at these two different methods and their affect on shape-controlled synthesis.

### 3.1. Homogeneous Nucleation

In homogeneous nucleation, seed formation proceeds according to the LaMer model (see Figure 4a), where reduction of metal ions occurs to generate a critical composition of atomic species in solution. Above this critical concentration, nucleation results in a rapid depletion of the reactants

 © 2008 Wiley-VCH Verlag GmbH & Co. KGaA, Weinheim 

small NANO MICRO

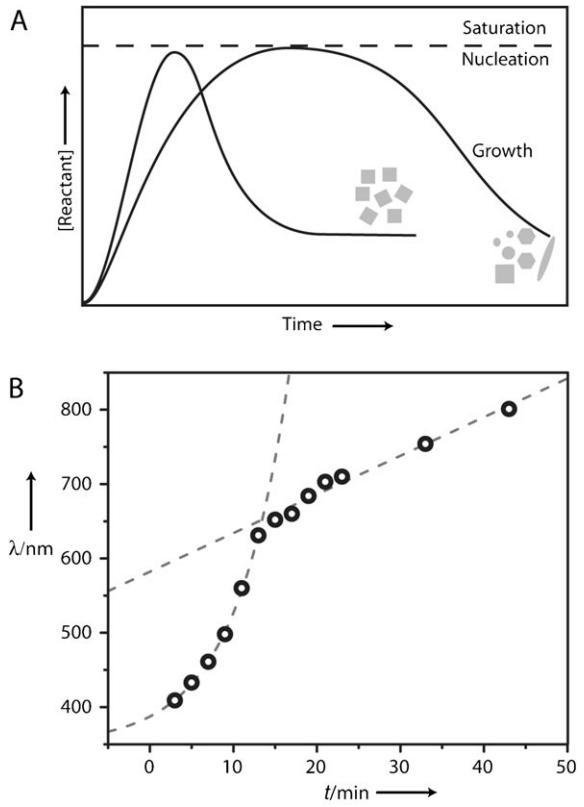


**Figure 4.** Nucleation and growth kinetics of metal nanoparticles. A) The La Mer model of nucleation, where a critical reactant concentration is required for particle nucleation. Homogenous nanoparticle dispersions are favored by a single, rapid nucleation event. B) Plot of reaction time versus dipolar surface plasmon wavelength, which is correlated to nanocrystal volume. Exponential nanocrystal growth corresponds to the nucleation process, whereas the linear regime corresponds to slow layer-by-layer growth (adapted from Reference [12]).

such that all subsequent growth occurs on the pre-existing nuclei. As long as the concentration of reactants is kept below the critical level, further nucleation is discouraged. This is particularly important for shape control: to obtain a highly shape-monodisperse yield of nanocrystals, nucleation must occur rapidly and instantaneously. This is exemplified by the synthesis of Ag nanocrystalline octahedra, whose reaction rate can be monitored by UV/vis spectroscopy (see Figure 4b). In other words, only a single nucleation event can occur. If nucleation is allowed to proceed over an extended period, reactants are unevenly depleted from solution leading to variations in growth rate for seed particles formed at different reaction times. Fast nucleation is typically achieved by slowly building up the concentration of metal ions in solution through serial injections of the precursor materials until nucleation occurs. However, preventing the fast reduction of metal ions – especially for colloidal syntheses carried out at reflux temperatures – is necessary to accumulate enough reactant species to reach the critical nucleation concentration. This accumulation may be aided by modifying the reactivity of the metal precursor. One possible method is through the formation of metal–surfactant or metal–polymer complexes in the reaction solution, which hinder the reduction reaction even under highly favorable conditions. For example, in the formation of polyhedral Pt nanocrystals, it is suggested that the coordination between $Pt^{2+}$ precursor and surfactant plays an important role.[36] For the formation of single-crystalline Ag nanocubes, a similar approach was taken to modify the solubility of the ionic precursor: the addition of trace amounts of $Cl^-$ to the reaction resulted in the precipitation of the low-solubility salt AgCl, preventing the immediate reduction of the metal ion.

Another condition required for homogeneous nucleation is that it must produce seed particles that are either single crystalline or that possess single-crystalline surfaces. For shape control, this is essential for controlling the subsequent growth of the nanocrystal. This is an especially difficult task for metals such as Ag, Au, Pt, and Pd, which exhibit a propensity for forming particles with a high degree of twinning; seeds with numerous crystal defects tend to result in polycrystalline nanoparticles with ill-defined morphologies. To prevent such particles from forming, homogeneous nucleation leading to shaped nanocrystals is often characterized by competing particle-forming and particle-dissolving reactions in solution. In the case of Ag nanocube and nanowire formation, Xia et al. have suggested that the presence of gaseous oxygen and chloride ions in the reaction mixture can oxidize and effectively etch particles that exhibit high-energy twin planes, resulting in the sole formation of single-crystalline particles. The presence of competing reduction and oxidation of Ag in the colloidal synthesis is further evidenced by the reversible nature of particle nucleation, observed empirically through a series of reversible color changes of the reaction solution. Similarly, for the formation of Ag nanocubes, cuboctahedra, and octahedra, the addition of trace amounts of $CuCl_2$ to the metal precursor solution also suggests the importance of coupled redox reactions. In the absence of $Cu^{2+}$, the $Ag^+$ reduction occurs upon the initial precursor injections to give unshaped, polycrystalline particles; addition of $Cu^{2+}$, which may serve as an oxidizer in the reaction, results in nucleation of single-crystalline particles after several injections of the Ag+ precursor have been added to the reaction pot.[12]

### 3.2. Heterogeneous Nucleation

In heterogeneous nucleation, the reaction conditions for shape control are less stringent given that seed particles are preformed in a separate synthetic step. In addition, the activation energy for metal reduction onto an already formed particle is significantly lower than for homogeneous nucleation of seed particles in solution.[37] As such, shape control can be considered as an overgrowth process: seed particles are added to a growth medium to facilitate the reduction of metal ions. Thus, utilizing heterogeneous nucleation for shape control allows a wider range of growth conditions that employ milder reducing agents, lower temperatures, or aqueous solutions. Murphy et al. have shown that the addition of preformed seeds to a metal precursor in the presence of a weak reducing agent effectively isolates the nucleation and growth events allowing control over the size and shape

 © 2008 Wiley-VCH Verlag GmbH & Co. KGaA, Weinheim 

of the resulting nanoparticles.[38,39] Small Au seeds, 3–5 nm in diameter, are added to a Au precursor solution containing ascorbic acid that is only capable of reducing the Au precursor in the presence of seeds. The resulting structures, rods and wires, as well as a variety of shapes,[40] can be synthesized by carefully controlling the growth stage, which is distinctly separate from the nucleation event. The reducing agent present in the growth step is only strong enough to induce autocatalytic growth on pre-existing nuclei.

If the seed particles possess well-defined shapes themselves, nanocrystal growth via heterogeneous nucleation can not only produce monodisperse nanocrystal sizes but can also influence (and in some cases template) the shape of the resulting nanocrystal after the final growth step. Gold nanoparticles as large as 18 nm effectively seed the growth of Au rods,[41] and Au rods themselves, either produced by electrochemical or chemical methods, have been used as substrates for overgrowth of both Au as well as other metals such as Ag and Pd).[13,42,43] In these cases, it is apparent that the shape of the seed affects the resulting overgrowth kinetics. For example, reduction of Pd on the {110} and {100} side facets of Au nanorods, as shown by Wu and co-workers,[42] exhibits competitive growth rates on the two facets where energy minimization dictates the dominance of {100} terminated Pd rods following overgrowth. Here, the surface structure of the seed determines the overgrowth morphology. Similarly, the overgrowth of Ag on multiple shapes of Au particles formed by the microwave polyol method indicates that the shape of the Au seed has a significant impact on the resulting binary crystal structure.[44] A dependence on surface structure has also been demonstrated by Mirkin et al. during the formation of Ag core/Au shell particles.[45]

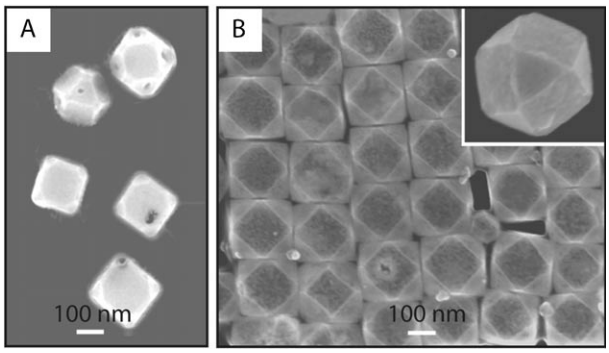


**Figure 5.** Seed-templated synthesis of nonspherical nanocrystals by galvanic displacement of Ag with Au. Ag nanocubes were incubated with aqueous solutions of $HAuCl_4^-$ to form hollow crystalline Au cuboctahedra, where the Ag crystal facets behave as epitaxial templates for displacement. In (A), the Au facets are not fully formed (adapted from Reference [3]).

As apparent in the examples listed above, for noble metal colloids the composition of the seed particle is not limited to the metal chosen for overgrowth. Carrying out nucleation and growth as separate synthetic steps allows the introduction of seed particles of one metal into a growth solution of a different metal. In fact, the choice of an alternative precursor for overgrowth can produce shapes and sizes that are inaccessible via homogeneous nucleation routes. For example, the adsorption and dissociation of $H_2$ on catalytically active Pt and Pd seeds has been demonstrated to catalyze the growth of Au, Pt, and Pd shells.[46,47] These core/shell nanostructures have been suggested to behave as more efficient catalysts for a variety of organic reactions due to favorable adsorption geometries and electronic considerations.[48] Hollow shell structures can also be obtained by carrying out nanocrystal growth using a metal ion exhibiting a higher reduction potential than the seed metal, with the inner surface of the shell retaining the shape of the seed (see Figure 5).[27,49]

More recently, seeded overgrowth of metal nanocrystals has been used to produce bimetallic heterostructures that exploit the epitaxial relationship between the two different metals, shown in Figure 6. Overgrowth of a secondary metal on well-faceted seeds enables the use of the crystallographic orientation of the seed to control metal reduction and growth of the secondary structure, producing anisotropic rods and polyhedra of Pd, Pt, and Au. For example, single-

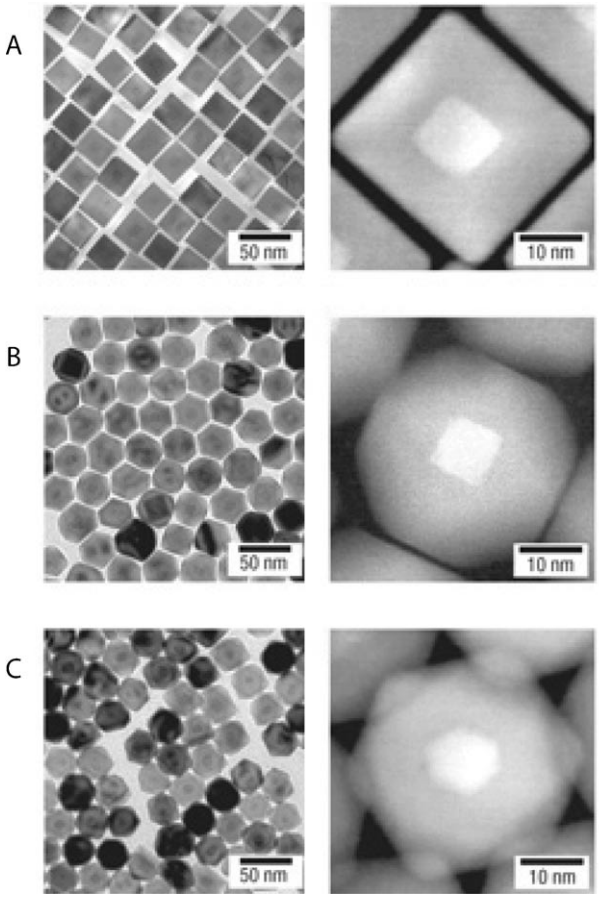


**Figure 6.** Highly faceted cubic Pt seeds can be used to control the morphology of a Pd shell. Transmission electron microscopy (left) and high-angle annular dark-field scanning transmission electron microscopy (right) images show the binary metal core/shell structure of overgrown Pd A) cubes, B) cuboctahedra, and C) octahedra (adapted from Reference [46]).

 © 2008 Wiley-VCH Verlag GmbH & Co. KGaA, Weinheim 

small NANO MICRO

crystalline Pd shells can be grown on cubic Pt seeds with an epitaxial interface, resulting in cubic core/shell structures.[50] This strategy draws on epitaxial gas-phase deposition of metals where, in the absence of alloy or compound formation, a thin film of a secondary metal can form in a layer-by-layer fashion. Growth can continue with the formation of three-dimensional (3D) islands by the Stranski–Krastanov mechanism or, alternatively, these islands can form at the outset of metal deposition via the Volmer–Weber growth mode.[51] For heteroepitaxy of metals in the solution phase, growth modes are not well understood and a high-level synthetic control is still necessary. While strongly influenced by the structure of the seed, nanocrystal growth is also subject to external shape-control factors including the nature of the surface-capping agent and various synthetic conditions of the growth step. Consequently, a faceted seed nanoparticle may define the epitaxial interface and initial growth pattern; however, shape-control chemistry in the growth step can be employed to further modulate the development of the final colloidal nanocrystal.

## 4. Nanocrystal Growth and Selective Adsorbates

For colloidal synthesis, shape control at the crystallographic level can be achieved by employing molecular capping agents that selectively adsorb to specific crystal planes. The general strategy to generate shape anisotropy during nanocrystal growth is by stabilizing a particular facet through this molecular interaction; growth is limited on the crystal plane where binding is strong and promoted on the crystal plane where binding is weak. For semiconductor and chalcogenide systems where different crystal planes are chemically distinct, this has been demonstrated by using mixtures of surfactants to achieve different polyhedral nanocrystals,[52] 1D structures,[14] and branched architectures.[53] For the fcc noble metals, the low-energy {111} and {100} facets possess similar surface energies and, thus, chemical reactivities; for Ag, these energies are 0.553 and 0.653 eV atom$^{-1}$, respectively.[54] Few molecules have been shown to possess selective binding preference between these two crystal planes, limiting the candidates for directing shape control. However, empirical synthetic experiments have shown a wide variety of molecules that can facilitate shape control, including large surfactants, polymers, and biomolecules, small molecules such as adsorbed gas, and even atomic species, such as different metal ions.

### 4.1. Surfactants

Early colloidal syntheses were characterized by the use of fluxional structures such as microemulsions,[55,56] micelles and vesicles,[57] and reverse micelles[58–60] that were postulated to behave as reactors or templates during synthesis. These so-called soft templates could be composed of a variety of molecules such as liquid crystals, block copolymers, and large biological molecules such as fatty acids. For the reduction of metal salts such as $HAuCl_4$ or $AgNO_3$, soft templating was typically carried out in an aqueous surfactant systems such as cetyltrimethylammonium bromide (CTAB), sodium dodecylsulfate (SDS), or bis(2-ethylhexyl) sulfosuccinate (AOT). Because they possess a hydrophilic head group and a hydrophobic tail, surfactants readily self-assemble into spherical or rodlike micelles in water, depending on concentration and the presence of other additives such as cosurfactants. Such structures were thought to promote metal reduction in or around the spatially confined hydrophilic volume. For instance, Au nanorods with aspect ratios of 2–10 were synthesized in the presence of CTAB and a cosurfactant, tetradodecylammonium bromide.[61] Cu nanoparticles and nanorods have also been demonstrated to form in AOT–water–oil systems, where shape can be controlled by changing the water–to–oil or salt concentrations of the reaction.[62] However, the role of the surfactant is difficult to elucidate. Charged surfactants often form complexes with the metal salt precursors, which may affect reduction kinetics.[63,64] In addition, because soft templates are dynamic in solution, it is unclear whether the surfactant assemblies are stable during the course of the reaction.[62] Although much work has been performed on these soft-template systems in past decades, the current prevailing thought among the materials research community is that these surfactants might not behave as a physical template for metal reduction but rather as growth-directing adsorbates on metal surfaces.

The difficulty in employing selective adsorption as a general synthetic method is the chemical specificity of these reactions: molecular adsorbates must be carefully chosen for a given crystal system. Because of their strong affinity for noble metals, molecules possessing a thiol functional group have been explored as nanocrystal capping agents. However, these molecules bind strongly to all crystal planes of these metals and promote the formation of spherelike, twinned nanoparticles with diameters of a few nanometers.[65,66] On the other hand, amines are only weakly bound to metal surfaces, several groups have explored nanocrystal synthesis using primary amines,[67] amine-terminated dendrimers,[68] and ammonium-terminated surfactants.[2,62,68] Particularly impressive shape control has been shown with the use of the latter surfactant systems, where encouraging a favored growth direction can yield anisotropic rods as well as bipod, tripod, and tetrapod Au nanostructures.[34] For many of these cationic surfactant systems, however, the relative importance of surfactant adsorption is unclear due to the presence of stabilizing anions and other metal ions present at low concentrations that may modify metal reduction. As in other nanoparticle syntheses, empirical results have done little to elucidate the shape-control mechanism.

### 4.2. Polyol Reaction

Perhaps the most successful reaction for producing noble metal colloids with controlled shape has been the polyol process employing the polymer poly(vinyl pyrrolidone) (PVP) as a surface-capping agent. Metal salt, the precursor for reduction, is dissolved in a polyol liquid that is

 © 2008 Wiley-VCH Verlag GmbH & Co. KGaA, Weinheim 

brought to near-reflux temperatures. Typical choices of polyols include ethylene glycol, 1,2-propylene glycol, and 1,5-pentanediol. Because viscosity ($\eta$) is largely determined by the length of the polyol's hydrocarbon chain (for the solvents listed, $\eta$ = 16.1, 40.4, and 140 mPa·s, respectively), choice of solvent can greatly impact diffusion and growth processes associated with metal nanocrystal formation. In addition, the polyol acts as the reducing agent for metal reduction and, at the relatively high temperatures for the reactions described herein, is likely oxidized to various aldehyde and ketone species. With an oxidation potential of 1.65 eV for ethylene glycol, metal reduction is much slower in the polyol process than for reactions that utilize strong reducing agents such as $NaBH_4$ that proceed to completion in a few minutes but is faster than photochemical reactions, which can take up to days for reactant consumption.

PVP is generally added at the start of the reaction or continuously during metal reduction. The role of the polymer is twofold: it acts as a stabilizing agent, preventing aggregation of metal particles and retaining a uniform colloidal dispersion. In addition, PVP is used as a shape-control agent or "crystal-habit modifier," promoting reduction onto specific crystal faces while preventing reduction onto others. For the noble metals, PVP has been demonstrated to stabilize the lowest-energy crystal facets of these fcc crystal systems to give colloidal structures bounded by {111}, {100}, and {110} planes. Although the actual mechanism for this selectivity is still under consideration, PVP is believed to bind preferentially to the {111} and {100} planes. Spectroscopic studies indicate that the PVP-metal interaction occurs through the carbonyl group of the pyrrolidone ring. This interaction has been empirically shown to be quite strong, with PVP replacement occurring only by the formation of a self-assembled monolayer (SAM) of alkanethiol. However, because adsorbate species on the surfaces of these metal colloids are difficult to resolve, it is unclear whether PVP has a stronger affinity for a particular crystal plane. In addition, it is difficult to elucidate whether PVP conformation plays a factor in the polyol process. Empirically, the polymer chain length significantly affects the shape and size dispersity of the synthesis and most literature gives optimized synthetic parameters for a PVP with an average molecular weight $M_w \approx 55\,000$.

Regardless, PVP has been demonstrated as an excellent shape-control agent for Ag,[3,12,15,69] Au,[15,69] Pt colloids,[13] and their alloys.[70] For each metal system, synthetic procedures have been developed for a variety of shapes that include rods, wires, cubes, octahedra, tetrahedra, icosahedra, and other polyhedra (Figure 7). These shapes are almost entirely bounded by {111} and {100} crystal facets. One-dimensional rods and wires are twinned nanostructures composed of multiple single-crystalline domains whereas polyhedral nanoparticles are almost exclusively single crystalline. For each of the three metal systems, a heterogeneous mixture of shapes and sizes can be obtained using the polyol process. Achieving homogeneous colloidal solutions requires optimization of reaction parameters, which include temperature, reactant concentrations, solvent viscosity, reaction time, reactant injection time and volumes, and the addition of ionic impurities the reaction flask. For Au, the polyol process is sensitive to the reactant concentration. For example, by changing the concentration of $HAuCl_4$, the salt used as the metal precursor, two different polyhedral shapes could be obtained: tetrahedra at high concentration and icosahedra at low concentrations.

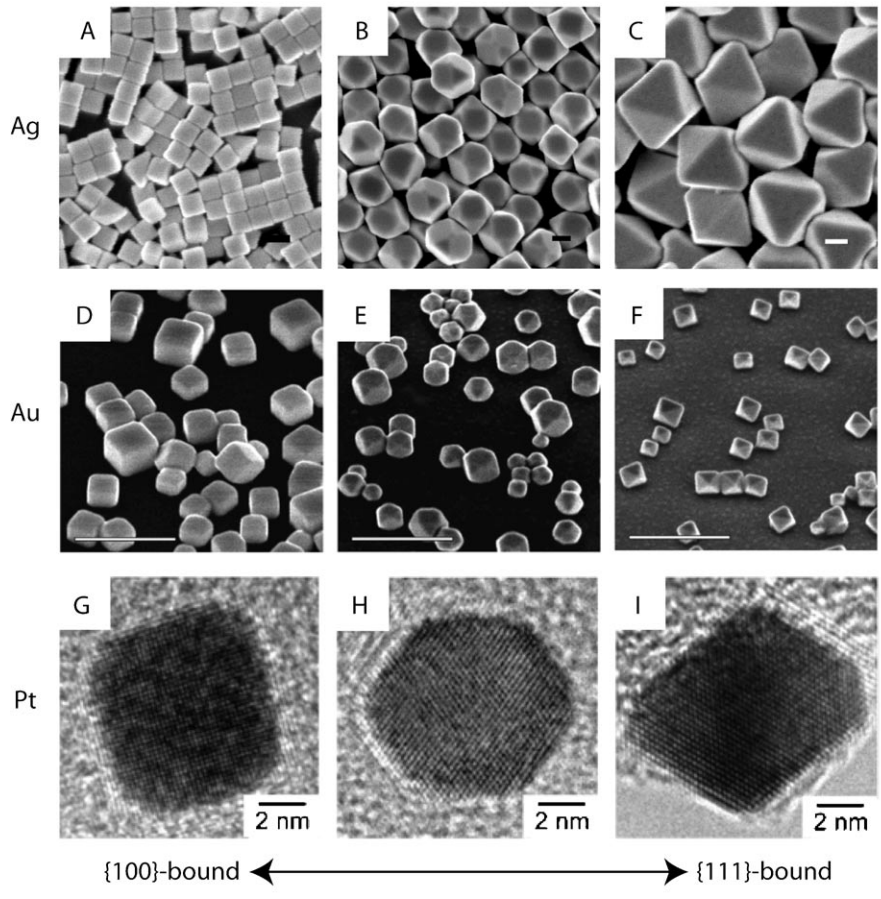


**Figure 7.** Polyhedral metal nanocrystals bound by the fcc {100} and {111} planes. Cubes, cuboctehedra, and octahedra have been obtained for silver (A–C, scale bar = 100 nm), gold (scale bar = 1 μm), and platinum (scale bar = 2 nm). The similarity between these noble metals suggests a general nucleation and growth mechanism where stabilization of the {111} facets relative to the {100} facets can be used to tune final nanocrystal shape (adapted from References [12–14]).

 © 2008 Wiley-VCH Verlag GmbH & Co. KGaA, Weinheim 

small NANO MICRO

For the synthesis of Ag colloids using the polyol process, shape control is achieved by controlling reaction kinetics. Reaction parameters are adjusted to: 1) promote fast nucleation and fast growth to form nanowires, or 2) fast nucleation and slow growth to form polyhedral nanocrystals (NCs), as depicted in Figure 8. For Ag nanowires, a low $[Ag^+]$:[PVP] ratio is used and the reaction proceeds with continuous injections of Ag nitrate into hot ethylene glycol. Upon nucleation of twinned Ag nanoparticles that act as seeds, nanowire growth occurs within a few minutes and it is difficult to isolate rods with aspect ratios $<10$.[30] For the NCs, a high $[Ag^+]$:[PVP] ratio is used and the reaction proceeds with continuous, simultaneous injections of Ag nitrate and PVP solutions in hot 1,5-pentanediol. The pentanediol, more viscous than ethylene glycol, slows reactant diffusion to encourage nucleation of single-crystalline particles over the multiply twinned particles, which initiate nanowire growth.[12] Nanowires, however, are still a byproduct of the reaction. NC growth can be continued for $\approx 2$ h to achieve large particles approximately 300 nm in diameter.

### 4.3. Small-Molecule and Atomic Adsorbates

Selective adsorption onto different crystal planes is not limited to large surfactants and long-chain polymers. In several instances, metal nanocrystal shape can be effectively modified by the addition of small molecules that exhibit the same preferential binding. During the heterogeneous overgrowth of Pd onto small Pt seeds, addition of $NO_2$ to the reactant solution has been demonstrated to stabilize the {111} faces of the resulting Pd nanocrystals with increasing ratios of $NO_2$ to Pd producing an increased ratio of {111} to {100} surface facets. Without $NO_2$, Pd nanocubes were produced; upon the addition of $NO_2$, Pd cuboctahedra and octahedra could be synthesized in high yield. Nitrogen dioxide, known to be a strong oxidizer, is thought to interact selectively with various Pd crystal planes, analogous to the chemical poisoning that occurs for Pt or Pd catalysts.[50]

Trace amounts of metal ions have also been used to achieve varying ratios of {111} to {100} nanocrystal facets. In the polyol reactions used to produce Au and Pt nanostructures, shape control was dependent on the addition of $AgNO_3$ to the reaction. The addition of a minute amount of Ag impurities (with $[Ag^+]$:$[Au^{3+}]$ approximately 1:100) produced a drastic effect, yielding homogenous colloidal solutions of Au nanocubes.[15] This foreign ion effect was systematically addressed for the case of Pt, where increasing the concentration of Ag impurities present in the reaction results in different NC shapes. With little ( $[Ag^+]$:$[Pt^{2+}]$ approximately 1:100) or no $Ag^+$ ions added to the Pt polyol reaction, nanocubes bounded completely by {100} facets are obtained; for increasing amounts of $Ag^+$ ions (1:10, 1:3), cuboctahedral and octahedral NCs were obtained, respectively. With increasing amounts of Ag, NCs bounded by larger areas of {111} facets could be obtained.[13] This suggests that for both the Au and Pt systems, $Ag^+$ ions may limit or enhance growth of particular crystallographic directions either through selective binding or galvanic-assisted reduction.

### 4.4. Bioinspired Routes

In a similar vein, other synthetic strategies have been explored utilizing the molecular recognition of biomolecules such as proteins and nucleic acids, which often contain various sulfide, amide, and carbonyl functional groups. The main advantage of these bioinspired routes is the existence of a huge molecular library, enabling a combinatorial approach to achieving nanocrystal shape control. For example, large libraries of peptides can be screened by attaching specific peptide sequences to microbeads, bacteria, or bacteriophages, incubating with the target surface, and recovering those sequences that exhibit crystallographic recognition. Using this technique, a library of $\approx 5$ million polypeptides with amino acid chains of 14 or 28 units was screened for specific binding affinities to metals such as Au or Cr.[71] Polypeptide sequences have been explored as Au binding agents that can catalyze specific growth directions to form thin platelets.[72] For Ag particles, biosynthetic routes where Ag-binding phage-display peptides are employed as shape-control agents have shown more success with producing well-faceted nanocrystals.[73] Size control of Cu nanocrystals has also been attempted using a histadine-containing peptide backbone, where conformational changes in the peptide can be correlated to the size dispersity of the nanocrystals.[74]

## 5. Applications for Shaped Metal Nanocrystals

### 5.1. Catalysis

The properties of noble metal nanocrystals make them ideal materials for application in catalysis, where reaction yield and selectivity are dependent on the nature of the cat-

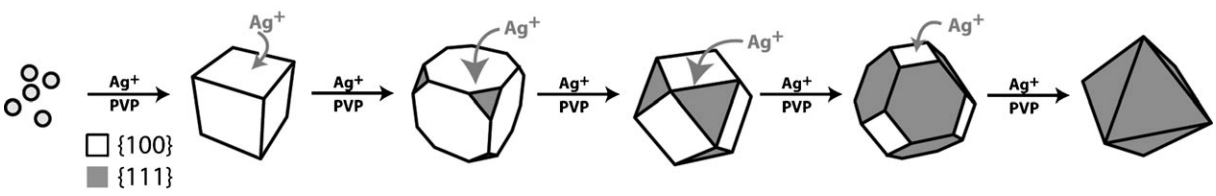


**Figure 8.** Polyhedral shape evolution of Ag nanocrystals. A schematic of the nucleation and growth processes, where silver continuously deposits onto the {100} facets to eventually result in a completely {111}-bound octahedron. By extending the polyol reaction for a given time period, various polyhedral shapes capped with {100} and {111} faces can be obtained in high yield (adapted from Reference [12]).

 © 2008 Wiley-VCH Verlag GmbH & Co. KGaA, Weinheim 

alyst surface. Because they possess a high surface-area-to-volume ratio compared to bulk materials, they have been found to exhibit higher turnover frequencies. More interestingly, however, is the application of shaped nanoparticles that possess single-crystalline surfaces as model heterogeneous catalysts. Key studies performed on bulk single-crystalline surfaces under ultrahigh vacuum (UHV) conditions have shown that certain reactions are structure sensitive, with a quintessential example given by the platinum-catalyzed hydrogenation of benzene: the (100) surface yields only cyclohexane while the (111) surface gives both cyclohexene and cyclohexane.[75] This dependence on surface structure can be naturally extended to nanocrystals bound by well-defined single-crystalline surfaces, particularly in the case of shape-controlled Pt, Pd, and Rh colloids. It has recently been shown that shape-controlled Pt nanocrystals with defined (100) and (111) surface structures exhibit benzene hydrogenation results that correlate well with single-crystal studies[75] (Figure 9). Here, the nanoparticles were assembled onto a planar solid support to form a 2D catalyst array ideal for monitoring gas-phase reaction intermediates by various spectroscopic techniques, enabling comparison with single-crystalline substrate work. Solution-phase studies, more traditionally within the domain of homogeneous catalysis, have also been undertaken using solutions of shaped colloidal nanoparticles. Reactions that have been investigated include cross-coupling, electron transfer, hydrogenations, and oxidation reactions. The electron-transfer reaction between hexacyannoferrate and thiosulfate has been catalyzed by Pt nanocrystals in the form of cubes, tetrahedra, and spheres.[76] Tetrahedral nanocrystals, completely bound by {111} crystal facets, exhibit the highest catalytic activity whereas cubic nanocrystals exhibit the lowest activity. However, it is still unclear whether this observation is truly a shape-dependent effect, as there is evidence that surface reconstruction and shape changes may occur in solution.[77] Direct surface measurements analogous to those commonly used for single-crystalline studies will need to be developed to study the dynamics of adsorbates on solution-phase nanocrystalline structures.

The largest obstacles facing shape-controlled nanocatalysis are compatible surface chemistry and shape retention. Ideally, fundamental catalytic studies should employ single-crystalline surfaces that are clean and well characterized. This is never the case for shaped colloidal particles, which, by nature of their synthesis, are protected by a layer of organic material. Although removing these stabilizing agents may be required to create accessible active sites, it is difficult to do so without inducing significant morphological change via surface reconstruction, particle ripening, melting, or oxidation. For heterogeneous catalysts supported on a solid substrate, ligand removal is presumed to occur with annealing at high temperatures. To elucidate whether this is a viable strategy, in situ TEM studies have been performed with colloidal metal nanocrystals heated to temperatures up to 800°C.[78,79] Removal of adsorbed capping molecules residual from the colloidal synthesis is observed at 250°C. Pt tetrahedra, cubes, and truncated cubes retain their shapes up to a temperature of ≈350°C, but experience rounding of their corners and edges at temperatures above 400°C; above 500°C, the particles undergo complete transformation into spherelike droplets on the solid support (Figure 10).

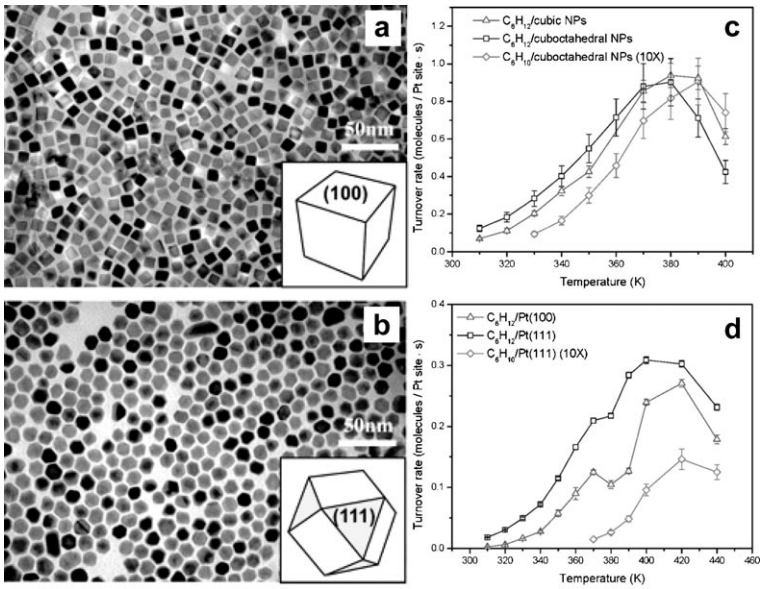


**Figure 9.** Shape-controlled Pt nanocrystals show catalytic selectivity for benzene hydrogenation. The turnover rate for films of surfactant-stabilized Pt A) cubes and B) cuboactahedra, shown in these TEM images, were measured. C) Cubic nanocrystals are selective for cyclohexane, while cuboctahedra exhibit activity for both cyclohexane and cyclohexene. These results are consistent with the selectivity exhibited by single-crystalline Pt surfaces, shown in (D) (adapted from Reference [71]).

### 5.2. Plasmonics

Subwavelength noble metal nanocrystals display a variety of unrivaled optical properties in the visible and near-IR regimes, including scattering cross sections orders of magnitude higher than the fluorescence emission from organic dyes and intense local amplification of electromagnetic fields. These phenomena result from localized surface plasmons (SPs), where the plasma oscillations of free electrons in the metal are bound by a finite volume given by the nanoparticle geometry. For noble metal nanocrystals, SP resonances are manifested as sharp maxima in the scattering intensity, which can be detected using traditional far-field optical methods such as

 © 2008 Wiley-VCH Verlag GmbH & Co. KGaA, Weinheim 

small

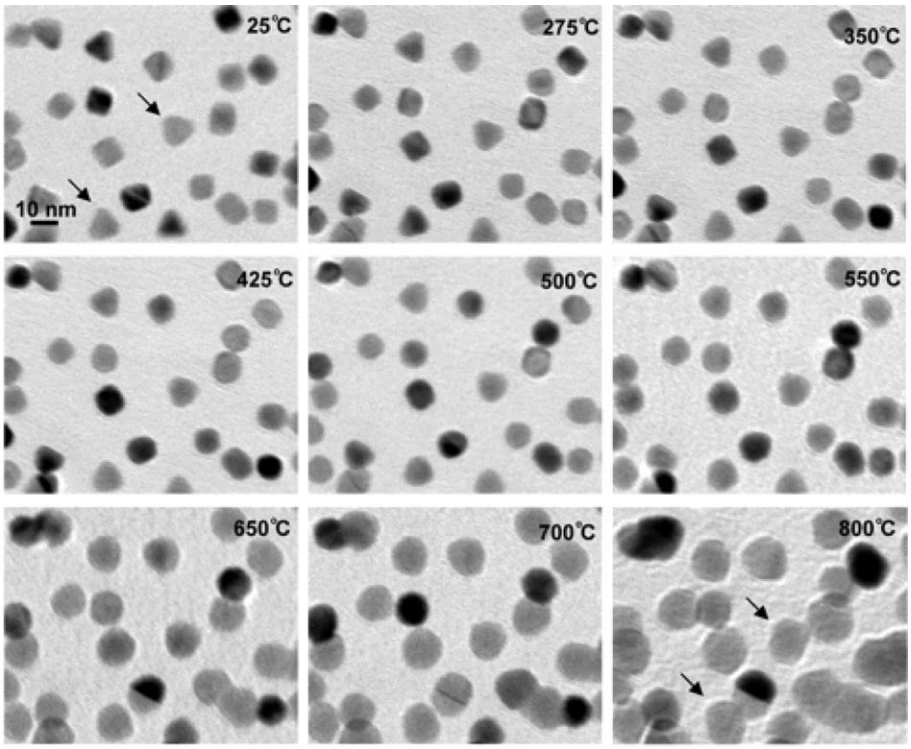


**Figure 10.** In situ shape transformation of nanocrystals. Pt nanocrystals immobilized on silica supports can be used as heterogeneous catalysts but undergo shape transformation and melting at the high temperatures required for several catalytic reactions. Above, in situ TEM images of a mixture of single-crystalline cubic and tetrahedral Pt nanocrystals. The nanocrystals are stable in shape and size until 350°C, after which the well-defined polyhedral shapes undergo significant truncation. After 500°C, aggregation and substrate wetting result in ill-defined, large particles with indistinguishable shapes (adapted from Reference [75]).

these lower-symmetry particle geometries would allow the possibility of tuning the plasmonic response with frequency and spatial resolution. We and others have shown that single metal nanocrystals of various shapes and sizes display unique scattering spectra based on their geometries, as shown in Figure 11.[12,85] A direct application of this scattering is the use of colloidal Au nanocrystals as imaging contrast agents specific to breast-cancer cells, generating large contrasts over a long period of time due to the nonexistence of photobleaching.[49] Because these plasmon resonances are sensitive to the dielectric surrounding of the nanocrystals, optical scattering measurements can be used to probe the chemical environment of the nanocrystal. Thus, the ability to engineer metallic nanocrystals that allow the excitation of specific SP modes would have profound consequences for applications that rely on electromagnetic-field enhancement, such as surface-enhanced Raman spectroscopy or plasmonic transport, where subwavelength metallic structures are used to guide light.

UV/Vis absorbance and dark-field scattering measurements. SP frequency, amplitude, and polarity are explicitly determined by the shape of the nanocrystal. For rodlike structures, Mie theory predicts a resonance peak associated with each respective axis, with increasing aspect ratios resulting in a larger energy splitting between the two resonances.[80] This length dependence has been demonstrated experimentally for both Au[2,81,82] and Ag nanorods[38,83] and is a prime example of how shape can be used to tune the optical properties of colloidal metal nanostructures.

Larger particles and particles with asymmetric shapes give rise to more complex SP responses due to their higher degree of polarizability. For example, six resonance modes are predicted for a cubic particle, with the majority of charge polarization localized at the corners and edges of the cube. In particular, a higher-order quadrupolar resonance mode is predicted to exhibit charge polarization almost exclusively at the corners of the cube.[84] Accessing

### 5.3. Surface-Enhanced Raman Spectroscopy

Because of its high sensitivity and chemical specificity, surface-enhanced Raman spectroscopy (SERS) has been demonstrated as a successful spectroscopic technique for

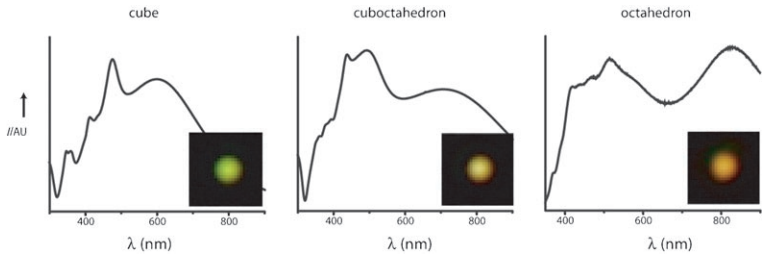


**Figure 11.** Shape-dependent optical response. UV/Vis spectra from colloidal dispersions of Ag nanocubes, cuboctahedra, and octahedra display distinct scattering signatures despite belonging to the same symmetry group. The insets show real color images taken with a digital camera displaying the different colors that result from plasmon-mediated scattering. Each spot is an image of a single nanocrystal; with increasing degrees of truncation, the color evolves from green to orange (adapted from Reference [12]).


© 2008 Wiley-VCH Verlag GmbH & Co. KGaA, Weinheim

low-level detection and analysis. Utilizing the electromagnetic-field enhancement associated with nanoscale metal surfaces, SERS intensities have been demonstrated to achieve the single-molecule detection limit.[86,87] These results have prompted a great deal of interest in SERS sensors for a variety of analytes, including biowarfare agents,[88] explosives,[89] small biological molecules such as glucose,[90] large proteins such as insulin,[91] DNA and single nucleotides,[92,93] and various hazardous environmental toxins[94] (Figure 12). In addition, SERS promises to be an advantageous technique for fundamental surface and interfacial studies, such as monitoring transport through biological membranes or the kinetics of charge-transfer at an electrode surface. Raman spectroscopy is a powerful tool for chemical analysis because it provides information about the vibrational signature of a molecule, which is sensitive to composition, bond strength, environment, and structure. Because SERS enhancement is inherently dependent on the light-scattering properties of the metal particle, choice of metal substrate and excitation wavelength are critical factors that influence observed Raman intensities.

Recent breakthroughs in the colloidal synthesis of metals have opened a new branch of SERS-active materials utilizing shape-controlled metal nanocrystals. In the past decade, a multitude of theoretical studies have examined electromagnetic-field enhancement with respect to nanoscale geometries, such as cylindrical wires,[95] wires with nonregular cross sections,[96] ellipsoids,[97] triangles,[1,98] and cubes[99] to name a few. This interest in nonspherical shapes stems from the observation of intense near-field enhancements localized around sharp vertices. Upon illumination with an incident field, charge polarization in the metal structure is maximized at these asymmetric features. Achieving such metal nanostructures experimentally with lithographic procedures is challenging, given fabrication limitations in the size regime of interest (10–100 nm). Colloidal chemistry, on the other hand, has demonstrated that specific shapes of Au and Ag nanoparticles can be synthesized in high yield and high uniformity.[1,3,12,15] Several studies have already demonstrated the efficacy of highly anisotropic nanorods[100–103] and nanowires[104–108] as SERS substrates, for both fundamental studies regarding near-field enhancements and in the construction of nanostructure junctions with exact arrangement (i.e., corner to corner, edge to edge). These shape-controlled colloids could provide increased SERS intensities by an order of magnitude and at the least could allow for the production of reliable, reproducible SERS-active substrates for sensing applications.

### 5.4. Bottom-Up Assembly

Shape-controlled nanocrystals have been long advertised as promising building blocks for novel materials. A general, robust method for colloidal assembly is the Langmuir–Blodgett (LB) technique, where 2D superlattices of colloidal structures are formed by pressure-induced organization at an air/water interface. Fluid-supported monolayers of nanoparticles or nanowires are subjected to isothermal compression and undergo phase transitions, proceeding from gas to liquid to solid as a function of increasing surface pressure.[89,109,110] The LB process is unique in its ability to achieve control over nanoscale order through tuning of a macroscopic property such as surface pressure. Under optimized conditions, it allows continuous tunability of particle density, spacing, and even arrangement (Figure 13). For metal nanocrystals with nonspherical shapes, superlattice assembly does not occur as readily as in the case for small ($<10$ nm) spherical colloidal particles. For larger Ag nanocrystals (diameter $d \approx 100$–$250$ nm), we demonstrated that interparticle separations could also be tuned to give electromagnetic coupling between nanoparticles.[109] Near-field interactions were observed for particles spaced as far as 40 nm apart and at shorter distances of $\approx 2$ nm, and can be completely delocalized over the entire nanocrystal monolayer. The

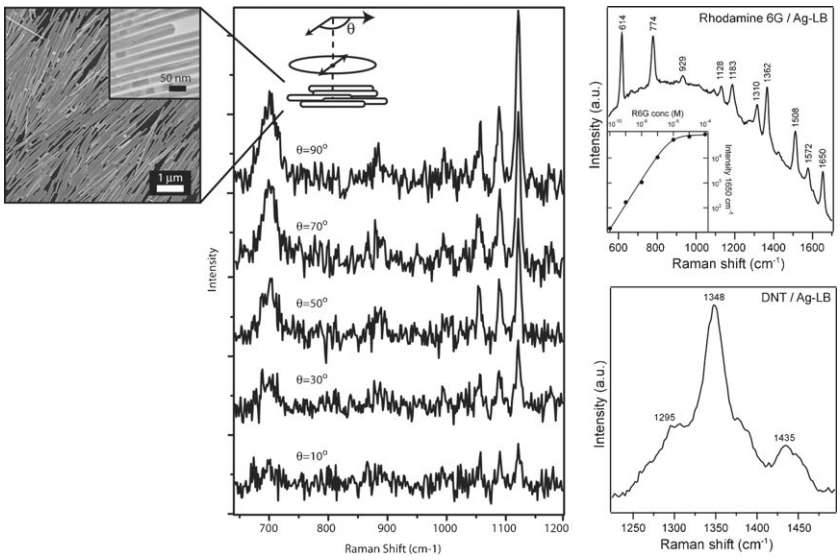


**Figure 12.** Chemical sensitivity of a silver nanowire SERS substrate. Left) SERS spectra of adsorbed 1-hexadecanethiol on a nanowire monolayer taken at different polarization directions of incident light. The angle is taken as the difference between the polarization direction and the long nanowire axis, as shown in the inset. The maximum SERS signal is collected with polarization orthogonal to the nanowire axis (adapted from Reference [96]). Right, top) SERRS spectrum of R6G on the thiol-capped Ag-LB film (532 nm, 25 mW) after 10 min incubation in a $10^{-9}$ M R6G solution. The inset shows the linear relationship between the Raman intensity at 1650 $cm^{-1}$ and the R6G concentration. Right, bottom) SERS spectrum of 2,4-DNT on the thiol-capped Ag nanowire monolayer after incubation for 10 min in $10^{-2}$ M 2,4-DNT/MeOH solution (adapted from Reference [85]).

 © 2008 Wiley-VCH Verlag GmbH & Co. KGaA, Weinheim 

NANO MICRO small

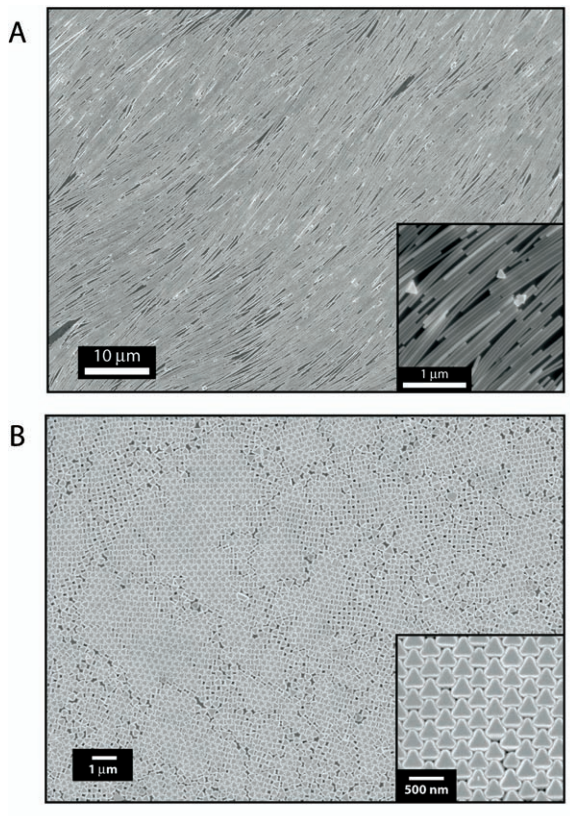


**Figure 13.** Large-scale Langmuir–Blodgett assembly of shaped metal nanocrystal building blocks. A) Silver nanowire monolayers adopt a nematic architecture resembling a liquid crystal (adapted from Reference [85]). B) Silver octahedra close packed into a hexagonal lattice forming an interlocked structure (adapted from Reference [97]).

observation of these co-operative effects demonstrate the LB technique as a powerful tool for constructing a large-scale, bottom-up material whose collective properties can be tuned by controlling organization at the nanoscale.

## 6. Summary and Outlook

Anisotropic, shaped nanoparticles are ideal building blocks for engineering and tailoring nanoscale structures for specific technological applications. Because noble metal nanocrystals were among the first materials to be utilized in controlled crystal growth in colloidal solutions, these systems are perhaps the most well understood in their general growth mechanism. Here, we have presented general guiding principles for the synthesis of well-defined shapes with single-crystalline surfaces. In addition, it is apparent from the wealth of shaped metal colloids discussed here that these systems comprise a large toolbox of nanostructures to utilize for application in photonics and spectroscopy, and as electrical or optical components in nanoscale devices. For such applications where morphology is key, metal nanocrystals have already begun to play an important if not integral role. For applications such as biomedical diagnostics and therapy or surface catalysis, control over surface chemistry is essential. It is highly likely that the distinct surface chemistries that these shaped particles offer can provide room for new directions in these fields. However, without directly probing the surface chemistry of these shaped metal nanocrystals, developments for these applications may remain elusive. More importantly for catalysis, shape control with precision $< 10$ nm effectively engineers the chemical surface of the nanoparticle. With this high degree of synthetic control, colloidal metal nanocrystals will most certainly have a profound impact in such scientific arenas as molecular biology, medicine, and catalysis, offering a highly tailored material from the micro- and nanoscale down to the molecular level.

## *Acknowledgments*

*This work was supported by the Division of Materials Sciences and Engineering, Office of Basic Energy Sciences, Department of Energy. A.R.T. is supported by the UC Office of the President Postdoctoral Fellowship.*

[1] R. Jin, Y. Cao, C. A. Mirkin, K. L. Kelly, G. C. Schatz, J. G. Zheng, *Science* **2001**, *294*, 1901.
[2] Y. Y. Yu, S. S. Chang, C. L. Lee, C. R. C. Wang, *J. Phys. Chem. B* **1997**, *101*, 6661.
[3] Y. Sun, Y. Xia, *Science* **2002**, *298*, 2176.
[4] T. S. Ahmadi, Z. L. Wang, T. C. Green, A. Henglein, M. A. El-Sayed, *Science* **1996**, *272*, 1924.
[5] P. A. Buffat, *Mater. Chem.Phys.* **2003**, *81*, 368.
[6] H. Hofmeister, *Cryst. Res. Technol.* **1998**, *33*, 3.
[7] J. W. M. Frenken, P. Stoltze, *Phys. Rev. Lett.* **1999**, *82*, 3500.
[8] C. L. Cleveland, U. Landman, T. G. Schaaff, M. N. Shafigullin, P. W. Stephens, R. L. Whetten, *Phys. Rev. Lett.* **1997**, *79*, 1873.
[9] J. K. Bording, B. Q. Li, Y. F. Shi, J. M. Zuo, *Phys. Rev. Lett.* **2003**, *90*, 22 6104.
[10] M. A. Van Hove, R. J. Koestner, P. C. Stair, J. P. Biberian, L. L. Kesmodel, I. Bartos, G. A Somorjai, *Surf. Sci.* **1981**, *103*, 189.
[11] N. Tian, Z.-Y. Zhou, S.-G. Sun, Y. Ding, Z. L. Wang, *Science* **2007**, *316*, 732.
[12] A. R. Tao, P. Sinsermsuksakul, P. Yang, *Angew. Chem.***2006**, *118*, 4713–4717; *Angew. Chem. Int. Ed.* **2006**, *45*, 4597.
[13] H. Song, F. Kim, S. Connor, G. A. Somorjai, P. Yang, *J. Phys. Chem. B* **2005**, *109*, 188.
[14] Y.-W. Jun, J.-S. Choi, J. Cheon, *Angew. Chem.* **2006**, *118*, 3492–3517; *Angew. Chem. Int. Ed.* **2006**, *45*, 3414.
[15] F. Kim, S. Connor, H. Song, T. Kuykendall, P. Yang, *Angew. Chem.* **2004**, *116*, 3759–3763; *Angew. Chem. Int. Ed.* **2004**, *43*, 3673.
[16] Y. Zhou, C. Y. Wang, Y. R. Zhu, Z. Y. Chen, *Chem. Mater.* **1999**, *11*, 2310.
[17] M. Maillard, S. Giorgio, M. P. Pileni, *J. Phys. Chem. B* 2003, 107, 2466.
[18] L. P. Jiang, S. Xu, J. M. Zhu, J. R. Zhang, J. J. Zhu, H. Y. Chen, *Inorg. Chem.* **2004**, *43*, 5877.
[19] F. Kim, J. H. Song, P. Yang, *J. Am. Chem. Soc.* **2002**, *124*, 14 316.
[20] Y. Zhou, S. H. Yu, C. Y. Wang, X. G. Li, Y. R. Zhu, Z. Y. Chen, *Adv. Mater.* **1999**, *11*, 850.
[21] A. L. Mackay, *Acta Crystallogr.* **1962**, *15*, 916.
[22] F. Baletto, C. Mottet, R. Ferrando, *Phys. Rev. B* **2001**, *63*, 155 408.

 © 2008 Wiley-VCH Verlag GmbH & Co. KGaA, Weinheim 

[23] Y. Xiong, J. M. McLellan, Y. Yin, Y. Xia, *Angew. Chem.* **2007**, *119*, 804; *Angew. Chem. Int. Ed.* **2007**, *46*, 790.
[24] K. Kwon, K. Y. Lee, Y. W. Lee, M. Kim, J. Heo, S. J. Ahn, S. W. Han, *J. Phys. Chem. C* **2007**, *111*, 1161.
[25] F. Baletto, R. Ferrando, *Rev. Mod. Phys.* **2005**, *77*, 317.
[26] A. Sánchez-Iglesias, I. Pastoriza-Santos, J. Pérez-Juste, B. Rodríguez-González, F. J. García de Abajo, L. M. Liz-Marzán, *Adv. Mater.* **2006**, *18*, 2529.
[27] Y. Sun, B. Mayers, T. Herricks, Y. Xia, *Nano Lett.* **2003**, *3*, 955.
[28] C. J. Johnson, E. Dujardin, S. A. Davis, C. J. Murphy, S. Mann, *J. Mater. Chem.* **2002**, *12*, 1765.
[29] S. Maksimuk, X. Teng, H. Yang, *Phys. Chem. Chem. Phys.* **2006**, *8*, 4660.
[30] B. Wiley, T. Herricks, Y. Sun, Y. Xia, *Nano Lett.* **2004**, *4*, 1733.
[31] J. D. Hoefelmeyer, K. Niesz, G. A. Somorjai, T. D. Tilley, *Nano Lett.* **2005**, *5*, 435.
[32] N. Zettsu, J. M. McLellan, B. Wiley, Y. Yin, Z.-Y. Li, Y. Xia, *Angew. Chem.* **2006**, *118*, 1310; *Angew. Chem. Int. Ed.* **2006**, 45, 1288.
[33] S. M. Humphrey, M. E. Grass, S. E. Habas, K. Niesz, G. A. Somorjai, T. D. Tilley, *Nano Lett.* **2007**, *7*, 785.
[34] S. Chen, Z. L. Wang, J. Ballato, S. H. Foulger, D. L. Carroll, *J. Am. Chem. Soc.* **2003**, *125*, 16 186.
[35] X. Teng, H. Yang, *Nano Lett.* **2005**, *5*, 885.
[36] H. Lee, S. E. Habas, S. Kweskin, D. Butcher, G. A. Somorjai, P. Yang, *Angew. Chem.* **2006**, *118*, 7988; *Angew. Chem. Int. Ed.* **2006**, 45, 7824.
[37] I. V. Markov, *Crystal Growth for Beginners: Fundamentals of Nucleation, Crystal Growth, and Epitaxy* **2003**, World Scientific Publishing Company.
[38] C. J. Murphy, N. R. Jana, *Adv. Mater.* **2002**, *14*, 80.
[39] N. R. Jana, L. Gearheart, C. J. Murphy, *Chem. Comm.* **2001**, 617.
[40] T. K. Sau, C. J. Murphy, *J. Am. Chem. Soc.* **2004**, 126, 8648.
[41] A. Gole, C. J. Murphy, *Chem. Mater.* **2004**, 16, 3633.
[42] Y. Xiang, X. Wu, D. Liu, X. Jiang, W. Chu, Z. Li, Y. Ma, W. Zhou, S. Xie, *Nano Lett.* **2006**, *6*, 2290.
[43] X. Kou, S. Zhang, Z. Yang, C. K. Tsung, G. D. Stucky, L. Sun, J. Wang, C. Yan, *J. Am. Chem. Soc.* **2007**, *129*, 6402.
[44] M. Tsuji, N. Miyamae, S. Lim, K. Kimura, X. Zhang, S. Hikino, M. Nishio, *Cryst. Growth Des.* **2006**, *6*, 1801.
[45] R. G. Sanedrin, D. G. Georganopoulou, S. Park, C. A. Mirkin, *Adv. Mater.* **2005**, *17*, 1027.
[46] P. N. Njoki, A. Jacob, B. Khan, J. Luo, C. J. Zhong, *J. Phys. Chem. B* **2006**, *110*, 22 503.
[47] Z. L. Wang, T. S. Ahmad, M. A. El–Sayed, *Surf. Sci.* **1997**, *380*, 302.
[48] G. Schmid, H. West, J.-O. Malm, J.-O. Bovin, C. Grenthe, *Chem. Eur. J.* **1996**, *2*, 1099.
[49] J. Chen, F. Saeki, B. J. Wiley, H. Cang, M. J. Cobb, Z. Y. Li, L. Au, H. Zhang, M. B. Kimmey, X. D. Li, Y. Xia, *Nano Lett.* **2005**, *5*, 473.
[50] S. E. Habas, H. Lee, V. Radmilovic, G. A. Somorjai, P. Yang, *Nat. Mater.* **2007**, *6*, 692.
[51] G. A. Somorjai, *Introduction to Surface Chemistry and Catalysis* Wiley, New York, **1994**.
[52] S. M. Lee, Y. W. Jun, S. N. Cho, J. Cheon, *J. Am. Chem. Soc.* **2002**, *124*, 11 244.
[53] L. Manna, E. C. Scher, A. P. Alivisatos, *J. Am. Chem. Soc.* **2000**, *122*, 12 700.
[54] L. Vitos, A. V. Ruban, H. L. Skriver, J. Kollar, *Surf. Sci.* **1998**, *411*, 186.
[55] C. T. Kresge, M. E. Leonowicz, W. J. Roth, J. C. Vartuli, J. S. Beck, *Nature* **1992**, *359*, 710.
[56] Y. Lu, R. Ganguli, C. A. Drewien, M. T. Anderson, C. J. Brinker, W. Gong, Y. Guo, H. Soyez, B. Dunn, M. H. Huang, J. I. Zink, *Nature* **1997**, *389*, 364.
[57] S. Link, M. B. Mohamed, M. A. El–Sayed, *J. Phys. Chem. B* **1999**, *103*, 3073.
[58] A. Taleb, C. Petit, M. P. Pileni, *Chem. Mater.* **1997**, *9*, 950.
[59] D. G. Shchukin, G. B. Sukhorukov, *Adv. Mater.* **2004**, *16*, 671.
[60] M. P. Pileni, *J. Phys. Chem. B* **1993**, *97*, 6961.
[61] N. R. Jana, L. Gearheart, C. J. Murphy, *J. Phys. Chem. B* **2001**, *105*, 4065
[62] M. P. Pileni, *Nat. Mater.* **2003**, *2*, 145.
[63] S. W. Kim, J. Park, Y. Jang, Y. Chung, S. Hwang, T. Hyeon, Y. W. Kim, *Nano Lett.* **2003**, *3*, 1289.
[64] B. L. Cushing, V. L. Kolesnichenko, C. J. O'Connor, *Chem. Rev.* **2004**, *104*, 3893
[65] M. Brust, M. Walker, D. Bethell, D. J. Schiffrin, R. Whyman, *Chem. Commun.* **1994**, 801.
[66] K. V. Sarathy, G. U. Kulkarni, C. N. R. Rao, *Chem. Comm.* **1997**, 537.
[67] D. V. Leff, L. Brandt, J. R. Heath, *Langmuir* **1996**, *12*, 4723.
[68] M. E. Garcia, L. A. Baker, R. M. Crooks, *Anal. Chem.* **1999**, *71*, 256.
[69] B. Wiley, Y. Sun, Y. Xia, *Acc. Chem. Res.* **2007**, *40*, 1067.
[70] J. M. Montejano-Carrizales, J. L. Rodríguez-López, U. Pal, M. Miki-Yoshida, M. José-Yacamán, *Small* **2006**, *2*, 351.
[71] S. Brown, *Nat. Biotech.* **1997**, *15*, 269.
[72] S. Brown, M. Sarikaya, E. Johnson, *J. Mol. Biol.* **2000**, *299*, 725.
[73] R. R. Naik, S. J. Stringer, G. Agarwal, S. E. Jones, M. O. Stone, *Nat. Mater.* **2002**, *1*, 169.
[74] I. A. Banerjee, L. Yu, H. Matsui, *PNAS* **2003**, *100*, 14 678.
[75] K. M. Bratlie, H. Lee, K. Komvopoulos, P. Yang, G. A. Somorjai, *Nano Lett.* **2007**, *7*, 3097.
[76] C. Burda, X. Chen, R. Narayanan, M. El-Sayed, *Chem. Rev.* **2005**, *105*, 1025.
[77] R. Narayanan, M. A. El-Sayed, *J. Phys. Chem. B* **2005**, *109*, 12663.
[78] Z. L. Wang, J. M. Petroski, T. C. Green, M. A. El-Sayed, *J. Phys. Chem. B* **1998**, *102*, 6145.
[79] R. Yu, H. Song, X. F. Zhang, P. Yang, *J. Phys. Chem. B* **2005**, *109*, 6940.
[80] G. C. Papavassiliou, *Prog. Solid State Chem.* **1979**, *12*, 185.
[81] B. M. I. van der Zande, M. R. Bohmer, L. G. J. Fokkink, C. Schonenberger, *J. Phys. Chem. B* **1997**, *101*, 852.
[82] M. B. Mohamed, K. Z. Ismail, S. Link, M. A. El-Sayed, *J. Phys. Chem. B* **1998**, *102*, 9370.
[83] V. M. Cepak, C. R. Martin, *J. Phys. Chem. B* **1998**, *102*, 9985.
[84] R. Fuchs, *Phys. Rev. B* **1975**, *11*, 1732.
[85] Y. Xia, N. J. Halas, *MRS Bull.* **2005**, *30*, 338.
[86] K. Kneipp, Y. Wang, H. Kneipp, L. T. Perelman, I. Itzkan, R. R. Dasari, M. S. Feld, *Phys. Rev. Lett.* **1997**, *78*, 1667.
[87] S. Nie, S. R. Emory, *Science* **1997**, *275*, 1102.
[88] C. L. Haynes, C. R. Yonzon, X. Zhang, R. P. V. Duyne, *J. Raman Spectrosc.* **2005**, *36*, 471.
[89] A. Tao, F. Kim, C. Hess, J. Goldberger, R. He, Y. Sun, Y. Xia, P. Yang, *Nano Lett.* **2003**, *3*, 1229.
[90] K. E. Shafer-Peltier, C. L. Haynes, M. R. Glucksberg, R. P. V. Duyne, *J. Am. Chem. Soc.* **2002**, *125*, 588.
[91] V. P. Drachev, M. D. Thoreson, E. N. Khaliullin, V. J. Davisson, V. M. Shalaev, *J. Phys. Chem. B* **2004**, *108*, 18 046.
[92] K. Kneipp, H. Kneipp, V. B. Kartha, R. Manoharan, G. Deinum, I. Itzkan, R. R. Dasari, M. S. Feld, *Phys. Rev. E* **1998**, *57*, R6281.
[93] L. R. A. D. L. S. Tuan Vo-Dinh, *J. Raman Spectrosc.* **2002**, *33*, 511.
[94] M. M. Mulvihill, A. Tao, P. Sinsermsuksakul, P. Yang, **2007**, unpublished results.
[95] J. P. Kottmann, O. J. F. Martin, **2001**, *8*, 655.

 © 2008 Wiley-VCH Verlag GmbH & Co. KGaA, Weinheim 

[96] J. P. Kottmann, O. J. F. Martin, D. R. Smith, S. Schultz, *Phys. Rev. B: Condens. Matt. Mater. Phys.* **2001**, *64*, 235402/1-235402/10.
[97] K. L. Kelly, E. Coronado, L. L. Zhao, G. C. Schatz, *J. Phys. Chem. B* **2003**, *107*, 668.
[98] J. E. Millstone, S. Park, K. L. Shuford, L. Qin, G. C. Schatz, C. A. Mirkin, *J. Am. Chem. Soc.* **2005**, *127*, 5312.
[99] L. J. Sherry, S.-H. Chang, B. J. Wiley, Y. Xia, G. C. Schatz, R. P. Van Duyne, *Nano Lett.* **2005**, *5*, 2034.
[100] C. J. Orendorff, L. Gearheart, N. R. Jana, C. J. Murphy, *Phys. Chem. Chem. Phys.* **2006**, *8*, 165.
[101] B. C. Stephen, S. Saratchandra, A. D. Richard, Y. P. Zhao, *Appl. Phys. Lett.* **2005**, *87*, 031 908.
[102] X. Hu, W. Cheng, T. Wang, Y. Wang, E. Wang, S. Dong, *J. Phys. Chem. B* **2005**, *109*, 19 385.
[103] G. H. Gu, J. Kim, L. Kim, J. S. Suh, *J. Phys. Chem. C* **2007**, *111*, 7906.
[104] S. E. Hunyadi, C. J. Murphy, *J. Mater. Chem.* **2006**, *16*, 3929.
[105] G. Sauer, G. Brehm, S. Schneider, H. Graener, G. Seifert, K. Nielsch, J. Choi, P. Goring, U. Gosele, P. Miclea, R. B. Wehrspohn, *J. Appl. Phys.* **2005**, *97*, 024 308.
[106] S. J. Lee, A. R. Morrill, M. Moskovits, *J. Am. Chem. Soc.* **2006**, *128*, 2200.
[107] A. R. Tao, P. Yang, *J. Phys. Chem. B* **2005**, *109*, 15 687.
[108] S. M. Prokes, O. J. Glembocki, R. W. Rendell, M. G. Ancona, *Appl. Phys. Lett.* **2007**, *90*, 093 105.
[109] A. Tao, P. Sinsermsuksakul, P. Yang, *Nat. Nanotechnol.* **2007**, *2*, 435.
[110] J. R. Heath, C. M. Knobler, D. V. Leff, *J. Phys. Chem. B* **1997**, *101*, 189.

Received: December 21, 2007

 © 2008 Wiley-VCH Verlag GmbH & Co. KGaA, Weinheim 